ELSEVIER

Observation of the Fracture Path Development in Mortar Beam Specimens

J. Davies
The University of Glamorgan, Department of Civil Engineering and Building, Mid Glamorgan, United Kingdom

The development of the fracture zone in beam specimens subjected to three-point and four-point bending has been observed and was related to the overall load-deflection relationship. A video technique together with the computer scanning facility were used to detect the initial macrocracks appearing before the attainment of the maximum load and also to record the fracture path formation in the postpeak portion of the load deflection curve. A comparison is made between unnotched and notched beams that are prepared for fracture testing from the standard size concrete beams. Due to its simplicity and cost effectiveness, this technique could be applied in many practical situations to detect the initial critical cracks and to reexamine the test results on the repetitive basis. ADVANCED CEMENT BASED MATERIALS 1996, 3, 31–36

KEY WORDS: Beam, Bending, Crack, Crack growth, Crack load, Fracture path, Mortar

Failures of cementitious materials involve a complex interaction that exists among its ingredients. Recent results of experiments carried out by several researchers [1–3], indicate that in coarse-grained materials a flexural type of crack face bridging develops primarily near aggregate particles.

The results of the mode I (tensile) fracture of concrete carried out by Van Mier [4] reveal that the fracturing of the specimens is a three-dimensional growth process. He suggested that the cracking starts from the outer layer of a specimen, most likely due to nonuniform drying out and the related tensile stresses near the specimen surface. The initial cracks that are generally bond cracks at the aggregate-paste interface, therefore, existed before the load was applied. It is generally accepted that the tensile fracture is characterized by a microcrack zone ahead of the macroscopic crack that is known as fracture process zone, but there is not direct proof of this as suggested by Mindess [5]. In spite of many attempts and modelings, it is not clear how to interpret this phenomenon to obtain a valid strength criteria for concrete-like materials.

The purpose of the work reported here was to contribute to the better understanding of the growth of the macroscopic cracks in beams during the loading process. Mortar beams were subjected to three-point and four-point bending regimes, and the progressive damage of the material was recorded on a high-quality videotape.

Experimental Investigation

Materials and Specimen Preparation

To focus on the local behavior of the fracture process zone and the macroscopic behavior of the beams with different geometries, we decided to use only one mortar mix throughout the whole investigation. Ordinary portland cement supplied locally conformed to BS 12:1973 and sea-dredged sand from Barry, South Wales, United Kingdom, which corresponded to zone 3, BS 882:1972, was dried thoroughly before batching. The ratio of cement:fine aggregates was 1:3, the water: cement ratio was kept to 0.5, and all samples were mechanically vibrated. The average compressive strength of the mix was 38 N/mm^2 [6].

Two different sizes of beam specimens were used throughout the experimental program. One type of beam geometry was prepared from 100 × 100 × 500-mm standard beams that were modified for the test purposes by cutting them into two identical halves 250-mm long and by inserting a notch. The other type was prepared from 75 × 75 × 200-mm purpose made beams. The beams were notched using a Clipper masonry saw fitted with a 253 mm diamond steel blade producing a notch of an average width of 1.5 mm. The accuracy of

Address correspondence to: J. Davies, Department of Civil Engineering and Building, University of Glamorgan, Pontypridd, Mid Glamorgan CF37 1DL United Kingdom.
Received May 31, 1994; Accepted March 17, 1995

ISSN 1065-7355/96/$15.00
SSDI 1065-7355(95)00042-P

Advn Cem Bas Mat
1996;3:31–36

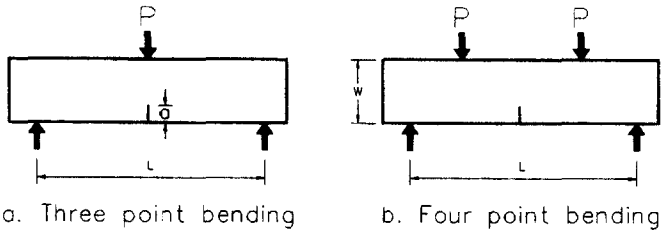

a. Three point bending b. Four point bending

FIGURE 1. Specimen geometry.

the notch insertion plays a major part in producing a consistent testing environment.

Experimental Setup

The wet-cured specimens were positioned in an Instron 8502 electro-hydraulic servo controlled testing machine with a maximum load capacity of 250 KN. The testing machine that complied with BS 1610:1985, clause 33, provided a digital display of load, and the load-deflection curves were plotted autographically. The tests were carried out at a room temperature of 20°C. In the displacement control mode, the cross head speed was kept at 0.003 mm/sec in all experiments.

The visual monitoring and the manual recording of the progressive damage were not sufficiently reliable to produce a realistic map of the fracture path development. To monitor, record, and study a fracture process in detail, a video image capture technique was used. A Panasonic VHS video camera fitted with an 8× power zoom lens set to 1/1000 shutter speed was mounted on the top of an adjustable tripod and positioned about 1 m in front of a sample. The camera was zoomed to a such extent that only a part of a ligament containing the crack was recorded. The videotape used during the study was a Sony CD VHS Extra HQ videocassette that was found sufficiently sensitive to record fine hairline cracks of about 0.01-mm wide in the mortar matrix.

Recordings of the experiments were analyzed by using MERLYN-X vision mixer with effects enabling us to split a fracture process into frames that were 1/25th of a second apart. The frames were frozen and then photographed from the video screen using a Pentax P30N still camera. Some shots were developed using a conventional photographic process and some were processed through a computer scanning program IMAGEIN installed on a Viglen 486 PC computer.

The detection of the initial microcracks that are associated with the fracture process zone appearing ahead of visible macrocracks is possible only if very sophisticated optical systems are used. It is known that a unique microcrack may develop before the maximum load is reached and without any clear indication on the load-deflection graph [1]. It is of great practical interest to be able to study the progressive damage of the material and to determine the load at which the first cracks appear in order to relate strength and cracking. The image capture method used in this investigation enabled us to relate the load-deflection response to the map of the fracture path.

Test Results

Three-Point Bending

The test arrangement is shown in Figure 1a: the larger beams with the effective span of 200 mm were notched with 20-mm slots and the smaller beams with the effective span of 150 mm were notched with 15-mm slots keeping depth: span and notch depth: depth ratio con-

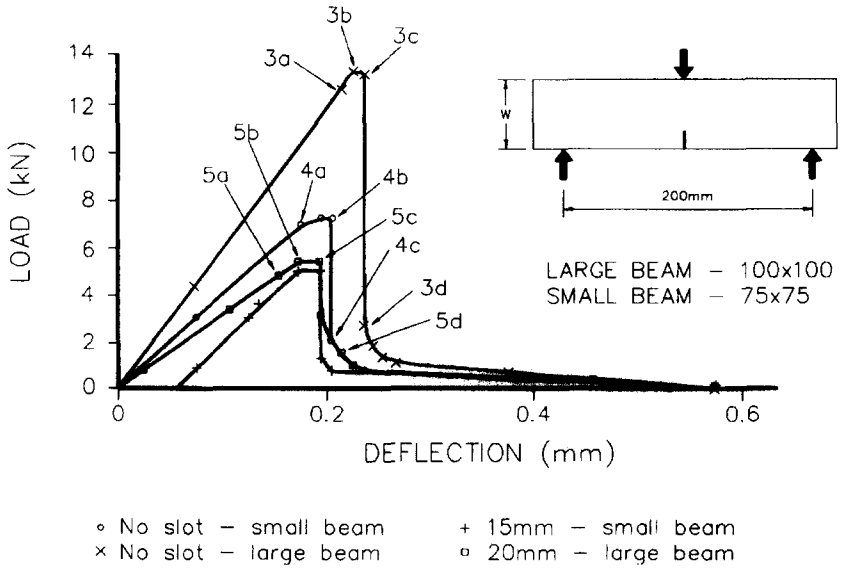

FIGURE 2. Load-deflection curves for three-point bending experiments. ○, No slot, small beam; X, no slot, large beam; +, 15 mm, small beam; □, 20 mm, large beam.

TABLE 1. Average test results of three-point bending experiments

Specimen Geometry (mm)	Notch Depth (mm)	First Crack Load (kN)	SD%	Maximum Load (kN)	SD%
75 × 75 × 200	0	7.05	19	7.28	16
	15	4.96	9	5.04	9
100 × 100 × 250	0	12.60	15	13.28	12
	20	5.40	12	5.48	7

stant and equal to w:L = 1:2 and a:w = 1:5, respectively. The beams were supported by a pair of 10-mm diameter steel rollers, and the load was applied through a 6-mm square bar.

Typical load-deflection curves for three-point bending experiments are shown in Figure 2, and the average tests results obtained from six experiments carried out on each beam geometry are given in Table 1.

A study of a progressive crack formation in the large unnotched beam is shown in Figure 3. The crack paths were obtained by the computer scanning and enhancement technique. In all six experiments, it was observed that the initial crack was a single vertical tortuous microcrack that appeared on the tensile side of the beam at about 97% of the maximum load. No other microcracks ahead of the crack tip were detected (Figure 3a and point 3a in Figure 2). This may be due to the fact that either the technique was not sensitive enough to detect them or they did not exist. With the increasing load, the initial crack began to open and subsequently another vertical discontinuous tortuous crack began to emerge in the ligament producing a frictional interlock or as it is sometimes called a crack bridging (Figure 3b and c and points 3b and 3c in Figure 2). The overlapping crack tips, which generally develop around stiff aggregates, hid behind each other, and the fracture process of the ligament between the crack tips became a stable process (Figure 3d and point 3d in Figure 2). After the bridge failure, the main single crack continued to open and propagate until the crack tip reached another bridge. This process continued until a complete failure of the sample was achieved. The final crack path was a single tortuous crack without any sign of crack branching, which propagated in almost vertical direction. This phenomenon was observed in both 75 × 75 × 200-mm and 100 × 100 × 250-mm beams.

Figure 4 shows a study of crack propagation in 75 × 75 × 200-mm beams with a 15-mm notch. It was apparent from the beginning that the crack interaction and linkages appeared to be denser than those observed in the unnotched specimens (Figures 4 a and b). This could indicate that the size of the crack linkages does not only depend on the aggregate size but also on the stress field in the ligament. Cracks initiate at one or both corners of the notch and eventually, under the increasing stress, the initial microcracks will interact and their size will be related to the localized stress field.

The final crack path was a single tortuous crack without any clear signs of crack branching. Relationship between a damage development and the load-deflection response is shown in Figure 2, points 4a, 4b, and 4c.

Figure 5 is a study of the crack development in a 100 × 100 × 250-mm beam with a 20-mm notch. The initial hairline crack developed in the almost vertical direction (Figure 5a and point 5a in Figure 2), and the subsequent discontinuous cracks emerged in a random manner along the length of the ligament (Figure 5b and point 5b in Figure 2). Some discontinuous microcracks physically closed during loading process and new micro-

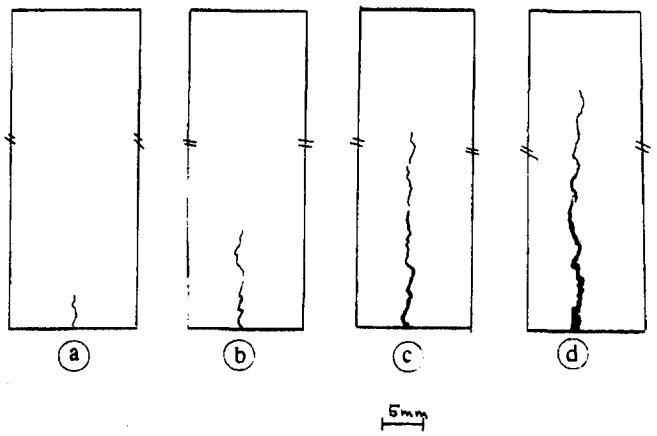

FIGURE 3. Crack-path formation in a three-point bending experiment with a 100 × 100 × 250-mm unnotched beam.

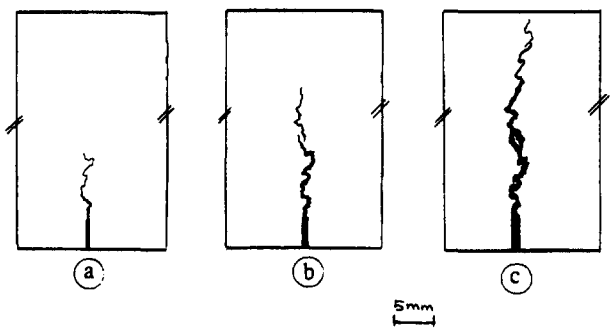

FIGURE 4. Crack-path formation in a three-point bending experiment with a notched 75 × 75 × 200-mm beam.

Advn Cem Bas Mat
1996;3:31-36

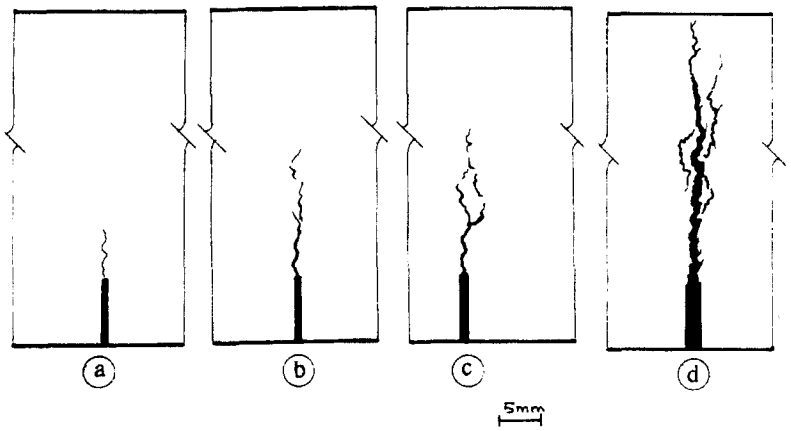

FIGURE 5. Crack-path formation in a three-point bending experiment with a notched 100 × 100 × 250-mm beam.

cracks developed at different locations (Figure 5c and point 5c in Figure 2), the final fracture path is shown in Figure 5d.

This phenomenon can be most probably attributed to either the formation of the superficial surface microcracks, which close as the surface strain field changes, or to the redistribution of stresses in the ligament that will allow some internal microcracks to reach the surface and produce new microcracks that would join the already existing damaged zone, or a combination of both.

Using the video technique and its ability to split the fracture process into the frames of 1/25th of a second apart, we could study the way these cracks moved during the loading process. This is demonstrated in Figures 5b, c, and d that have a time lag of about 20 seconds between them.

It can be seen that the amount of discontinuous cracks increased with the increasing deflection and, apart from a clearly defined main crack, a number of parallel tortuous cracks accompanied the main crack path. The crack linkages or facing bridges appeared larger than those in smaller beams, indicating that their size most probably depends on overall stress field. The similar phenomenon was observed by the author during the mixed mode experiments [7].

Four-Point Bending Setup

The test arrangement is shown in Figure 1b, the load spacing for the larger beams was kept at 100 mm, and for the smaller beams it was kept at 75 mm. The same ratios of depth:span and notch depth:depth have been used as described in the three-point bending experiments. The test results shown are the average values obtained from six experiments carried out on each beam geometry and the notch arrangements. Table 2 is a summary of the average first crack and maximum loads. Figure 6 shows typical load deflection curves for the beams.

Figure 7 shows photographs of the overall map of the crack development in 75 × 75 × 200-mm beams. A crack path is considerably inclined, and there are signs of a crack branching at the tip of the crack. The cracking process is related to the load-deflection response in Figure 6 by points 7a, 7b, and 7c.

Figure 8 depicts a typical crack development as observed in 100 × 100 × 250-mm beams (points 8a and 8b in Figure 6). The crack path was less curved and the singular inclined cracks appeared within the ligament. These cracks grew with the increasing stress until their length reached the state of mechanical instability followed by macroscopic fracture and failure. Figure 8 represents an overall map of damage.

Conclusion

Three-point and four-point bending experiments were carried out on the unnotched and notched mortar beams to study the relation of damage and loading. The results presented here are based on six experiments for each beam geometry.

TABLE 2. Average test results of four-point bending experiments

Specimen Geometry (mm)	Notch Depth (mm)	First Crack Load (kN)	SD%	Maximum Load (mm)	SD%
75 × 75 × 200	0	7.82	12	10.75	16
	15	5.74	9	8.10	11
100 × 100 × 250	0	15.68	14	23.20	10
	20	10.60	11	13.13	9

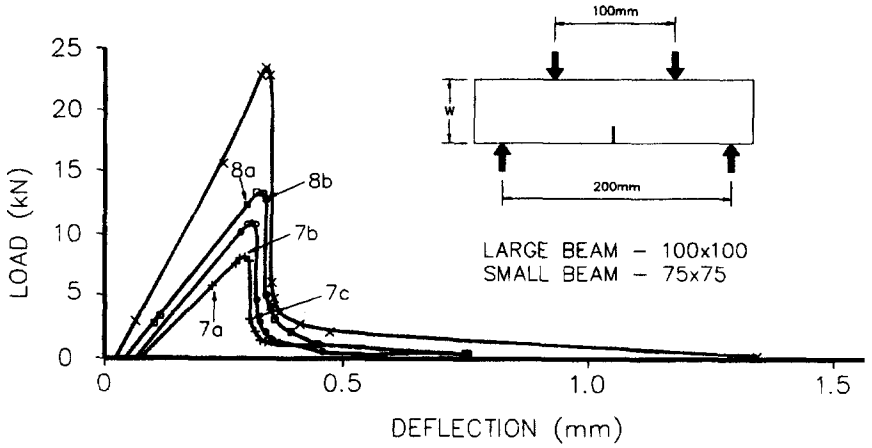

FIGURE 6. Load-deflection curves for four-point bending experiments. ○, No slot, small beam; X, no slot, large beam; +, 15 mm, small beam; □, 20 mm, large beam.

The experimental work described here aimed to provide information about the interaction and linkage of cracks leading to macroscopic fracture and failure. To provide a physically more realistic description of fracture development, a video technique together with the computer scanning facility was used. The main advantage of this method is its simplicity and low cost. It is suggested that the observed crack damage develop-

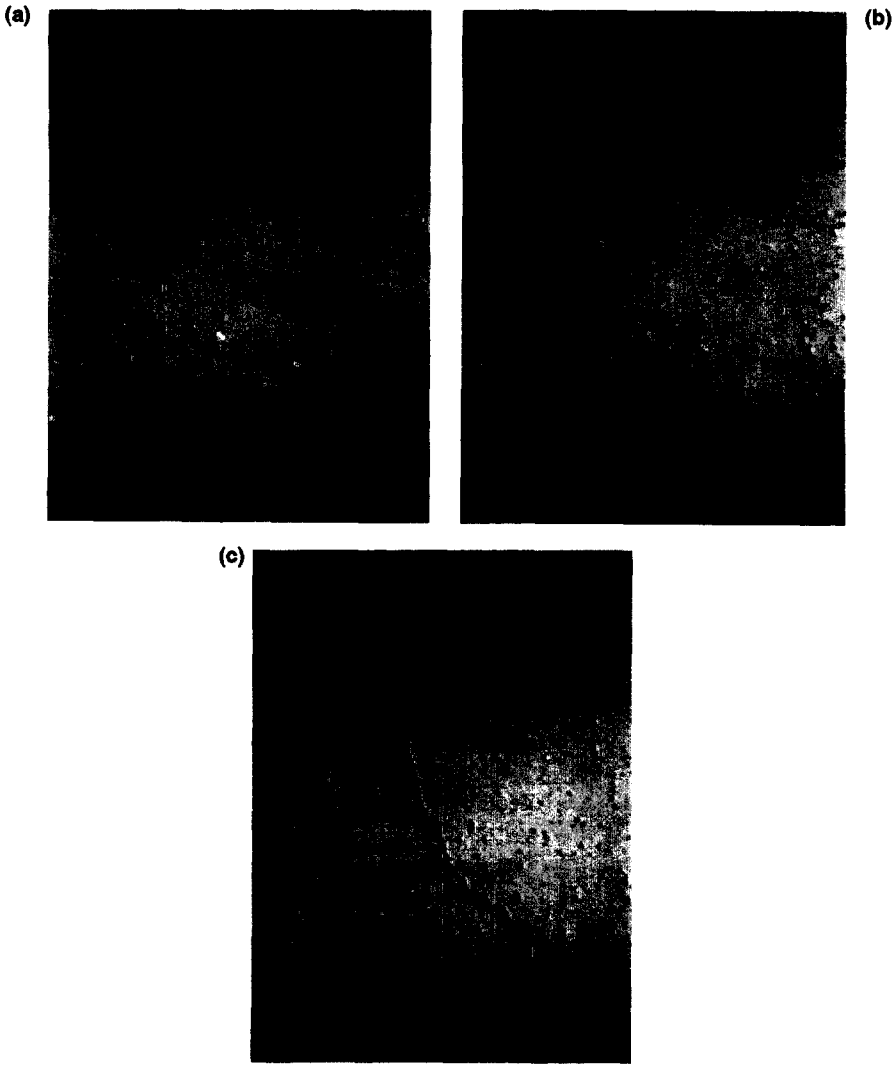

FIGURE 7. Crack-path development in a four-point bending experiment with a 75 × 75 × 200-mm beam.

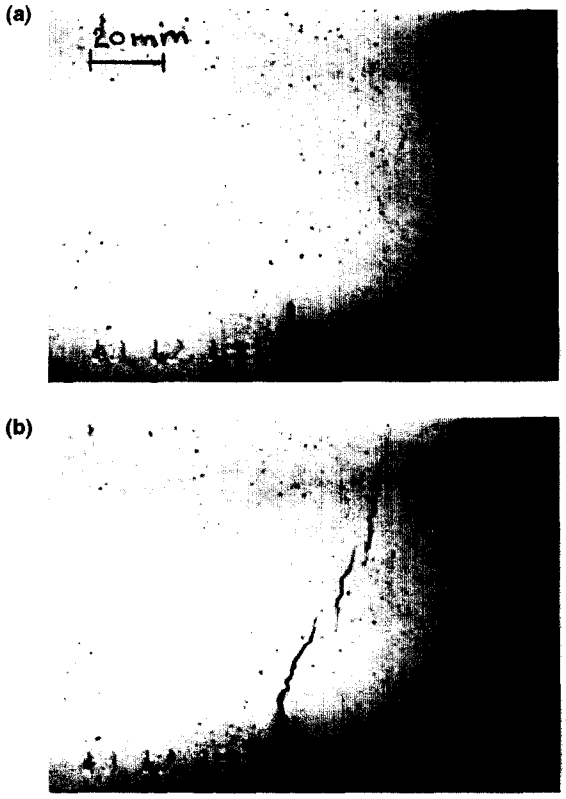

FIGURE 8. Crack-path development in a four-point bending experiment with a 100 × 100 × 250-mm beam.

ment provides additional information regarding the evolution of cracks in mortar beams subjected to bending. It must be realized that the accuracy of the observed process zone depends significantly on the sensitivity of the equipment.

Acknowledgment

The author wishes to express thanks to Mr. P.G. Bakar and the Media Resources Unit at the University of Glamorgan for their help and patience during the data analysis.

References

1. Bascoul, A.; Turatsinze, A. In *Fracture Mechanics of Concrete Structures;* Bazant, Z.P., Ed.; Elsevier Applied Science, 1992.
2. Van Mier, J.G.M. In *Fracture Processes in Concrete, Rock and Ceramics;* Rilem, 1991; pp 27–39.
3. Schlangen, E.; Van Mier, J.G.M. In *Fracture Processes in Concrete and Rock,* vol. 2; E & FN Spon, 1991; pp 705–716.
4. Van Mier, J.G.M. *Cem. Concr. Res.* **1991,** *21,* 1–15.
5. Mindess, S. In *Fracture Mechanics of Concrete-Test Method;* RILEM TC—89 FMT, 1991.
6. Bakar, P.G. *The Study of Crack Propagation in Cementitious Materials* [Internal Report]; University of Glamorgan, 1992.
7. Davies, J. In *Fracture Mechanics of Concrete Structures;* Bazant, Z.P., Ed.; Elsevier Applied Science, 1992; pp 713–771.